

Supporting information

**Poly(3,4-ethylenedioxythiophene)/ Nickel Disulfide Microspheres Hybrid in
Energy Storage and Conversion Cells**

Radha Mukkabl,^a Melepurath Deepa,^{a} and Avanish Kumar Srivastava^b*

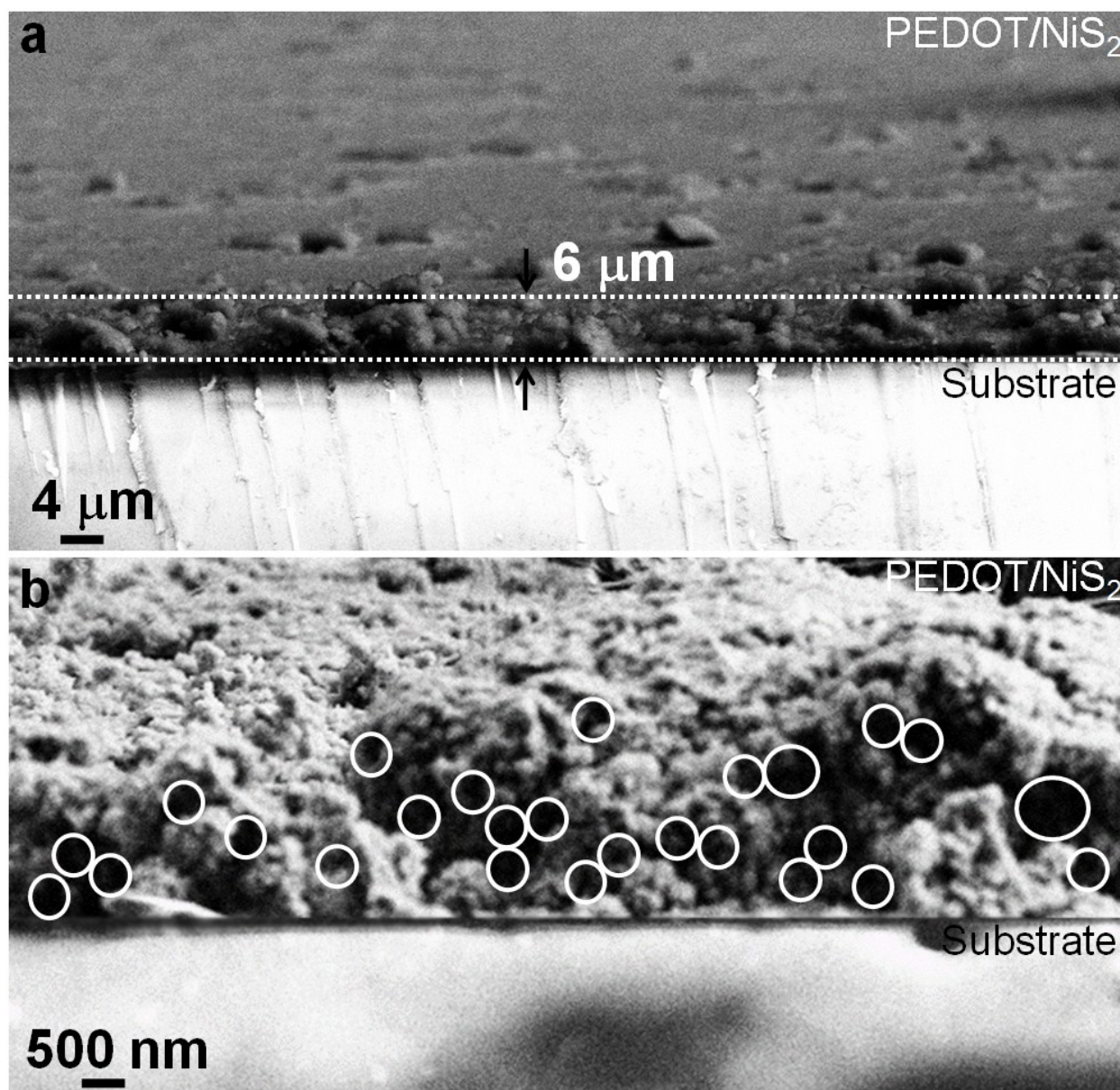


Figure S1 (a) Low and (b) high magnification cross-sectional FE-SEM images of an electrodeposited PEDOT-NiS₂ hybrid film. The solid circles in (b) enclose the pores in the film.

Supporting information

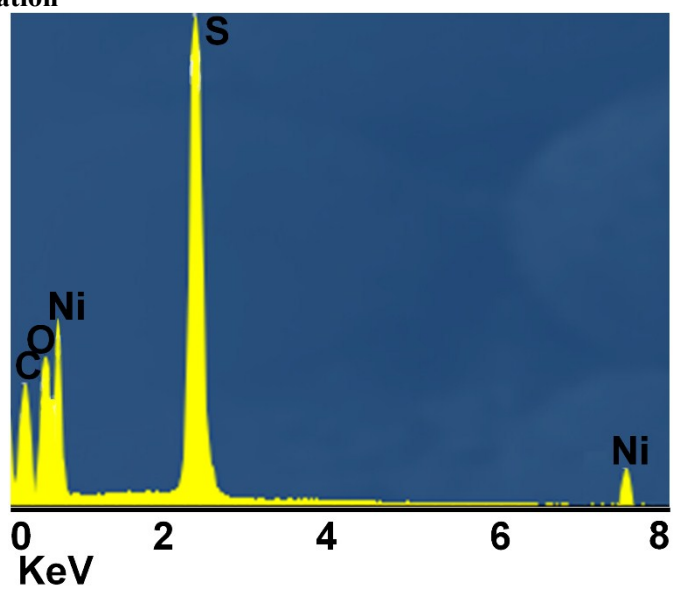


Figure S2 Energy dispersive X-ray (EDX) analysis plot of the PEDOT/NiS₂ hybrid.

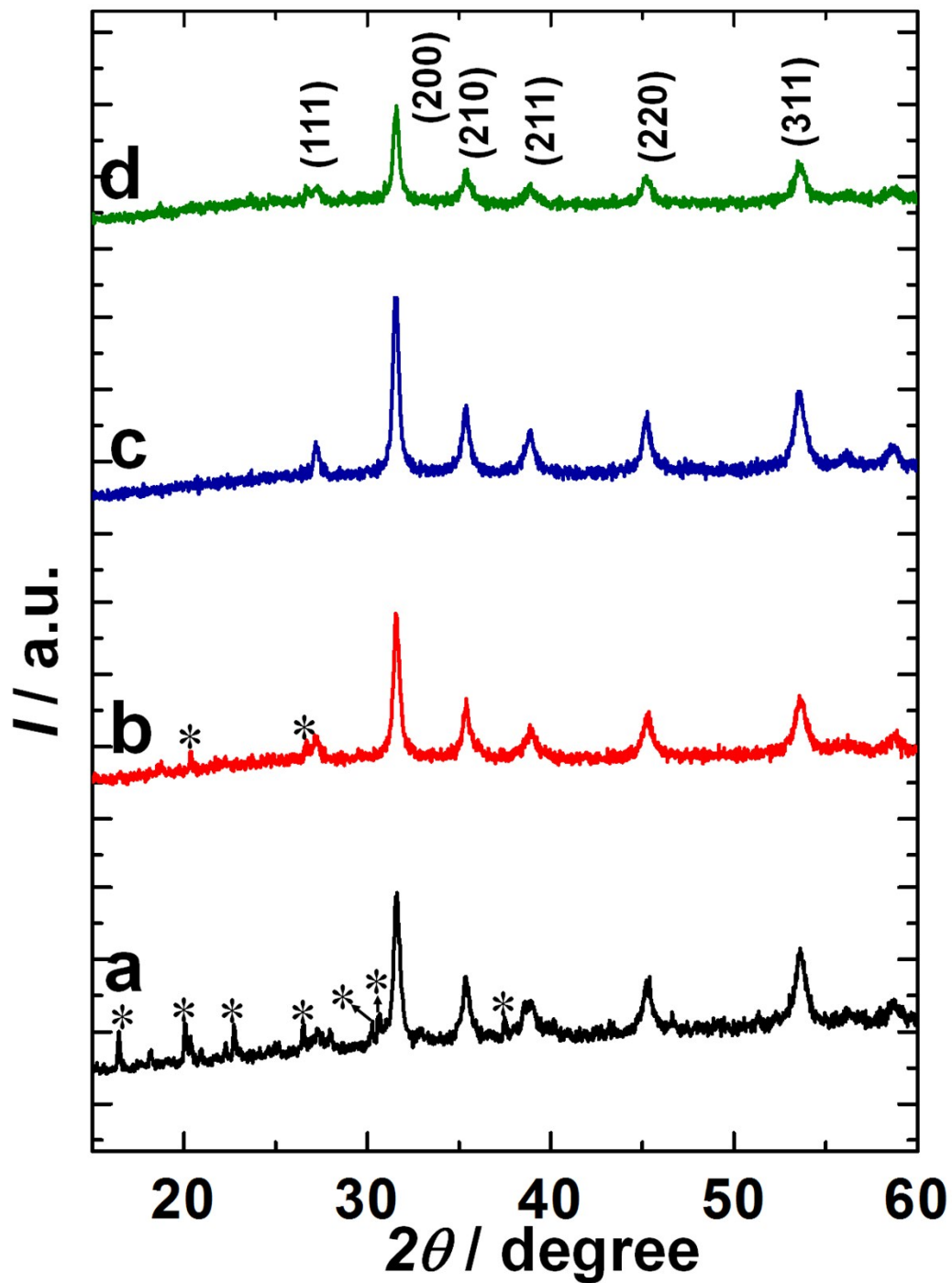


Figure S3 XRD patterns of NiS₂ samples, obtained after heating an aqueous solution of 2.5 mM of NiCl₂ · 6H₂O and 2.5 mM Na₂S₂O₃ · 5H₂O at (a) 120 °C, (b) 140 °C, (c) 150 °C and (d) 160 °C for 12 h, under hydrothermal conditions. The asterisk marked peaks correspond to impurities.

Supporting information

Symmetric cells were constructed in the NiS₂-NiS₂ configuration with an electrolyte soaked separator affixed between the two layers. The cyclic voltammograms of symmetric cells of pristine NiS₂ (supported on both rigid (SS foil) and flexible (C-fabric) current collectors) were recorded at different scan rates of 2, 5, 10, 20, 50 and 100 mV s⁻¹ in the voltage window of -0.2 to +0.6 V (Figure S4a and b). The CV profiles of the NiS₂ based rigid and flexible cells show a leaf like shape, at all scan rates. The capacitive characteristics of pristine NiS₂ are poor, and this is also reflected in the charge-discharge plots. Galvanostatic charge discharge curves of the pristine NiS₂ based symmetric cells supported on both SS foil and C-fabric, measured at current densities of 2, 4, 6, 8, 10 A g⁻¹ are shown in Fig S4d and e respectively. The SC decreased from 9 F g⁻¹ to 2.5 F g⁻¹ for the rigid SS cells and it is dropped from 16 F g⁻¹ to 40 F g⁻¹ when the current density was increased from 2 to 10 A g⁻¹ for the flexible C-fabric cells, with pristine NiS₂ as the active layer. The dismal performance of pristine NiS₂ cells is attributed to two factors. (i) The adhesion of pristine NiS₂ with the current collector is poor and the active material peels off during electrochemical cycling, and (ii) the redox reactions of NiS₂ are kinetically slow. The cycling stability of pristine NiS₂ based rigid and flexible symmetric supercapacitors, recorded at the same current density of 10 A g⁻¹ over 1500 cycles are shown in Fig S4e and f. The flexible symmetric cell exhibits better capacity retention and higher SC values compared to its' rigid symmetric counterpart. The flexible and the rigid symmetric cells show 19% (22 F g⁻¹) and 92% (32 F g⁻¹) capacity retention at the end of 1500 cycles respectively. The better performance of the flexible cell is due to the porous rough microstructure of the C-fabric, compared to the planar, smooth surface of the SS foil. The NiS₂ microspheres therefore, adhere more strongly to the C-fabric compared the foil, which results in a higher SC for the cells supported on C-fabric.

Supporting information

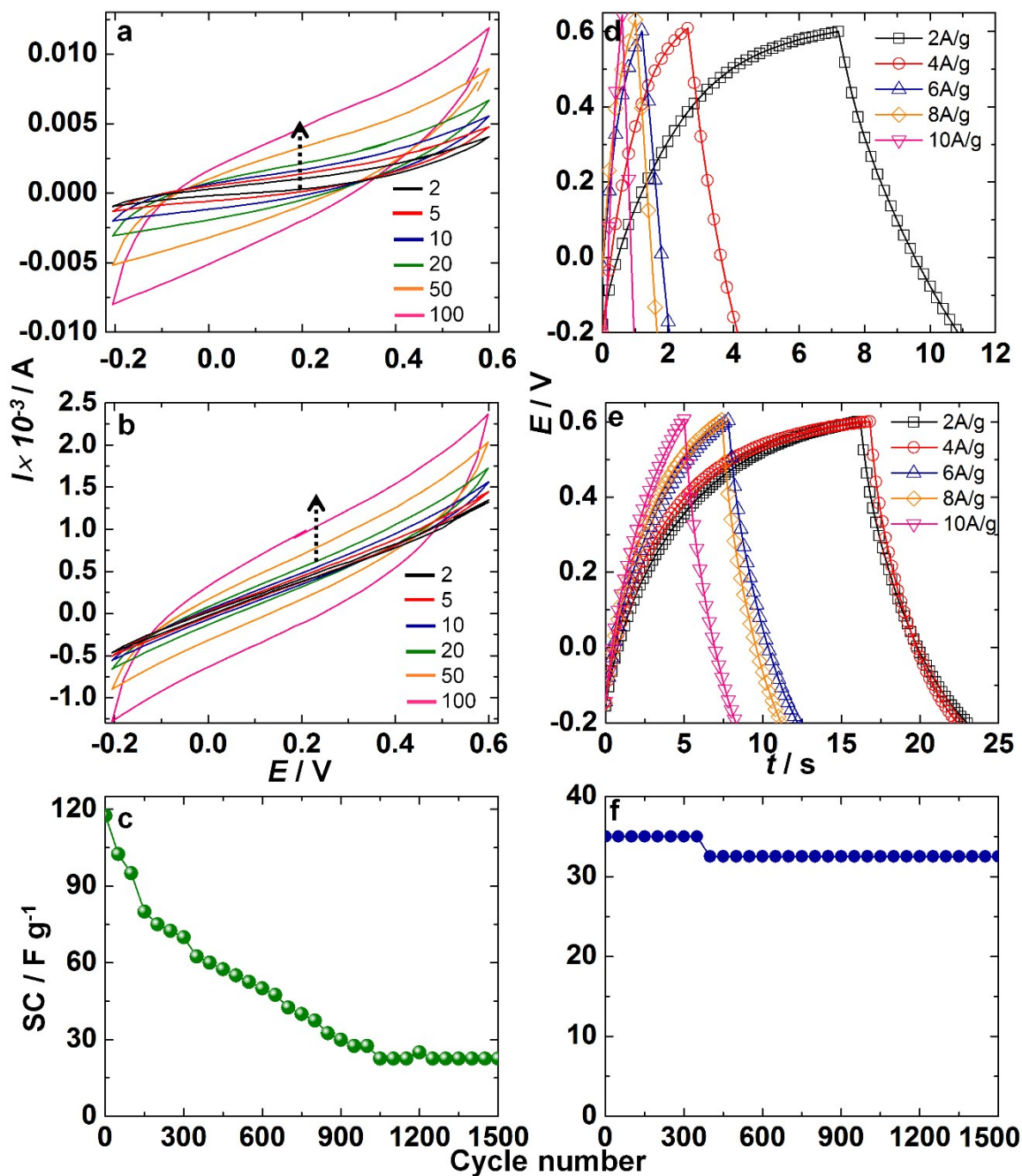


Figure S4 Comparison of CV plots of NiS₂-NiS₂ based symmetric cells supported on (a) rigid (SS) and (b) flexible (C-fabric) current collectors recorded at different scan rates of 2, 5, 10, 20, 50 and 100 mV s⁻¹. Comparison of galvanostatic charge-discharge characteristics of NiS₂-NiS₂ based symmetric cells supported on (d) rigid and (e) flexible current collectors recorded at 2 (●), 4 (○), 6 (□), 8 (✱) and 10 (♦) A g⁻¹. Specific capacitance variation as a function of number of charge-

Supporting information

discharge cycles recorded at a current density of 10 A g^{-1} , for symmetric NiS_2 - NiS_2 based cells supported on (c) rigid and (f) flexible current collectors.

Construction of quantum dot solar cells (QDSCs) and characterization:

A lump-free TiO_2 (anatase phase, particle size $< 25 \text{ nm}$, Aldrich) dispersion was prepared in ethanol, by mixing TiO_2 (1 g) in ethanol (5 mL). The resulting white suspension was applied on FTO coated glass using a doctor blade method and annealed at $150 \text{ }^\circ\text{C}$ for 40 minutes for solvent removal and attachment of TiO_2 to the substrate, followed by an annealing at $500 \text{ }^\circ\text{C}$ for 1 h. CdS quantum dots (QDs) were deposited on the TiO_2 coated FTO plates by a successive ionic layer absorption and reaction (SILAR) method. The TiO_2 /FTO electrode was consecutively immersed in four different beakers for about 30 s soaking time, in each solution. The first dipping solution was composed of aqueous $\text{Cd}(\text{CH}_3\text{COO})_2$ (0.1 M, Merck) which, was followed by a deionized water rinse to remove the excess acetate. The film was then submerged in aqueous Na_2S (0.1 M, Merck), and again followed by a water dip to remove the surplus sulfide. The immersion cycle was repeated seven times. The resulting films were yellow and were referred to as CdS/ TiO_2 electrodes. PEDOT/ NiS_2 and PEDOT films were deposited on FTO coated glass substrates by potentiostatic electropolymerization ($E = 1.5 \text{ V}$ for 600 s) from their respective precursor solutions containing (a) 0.1 M EDOT + NiS_2 spheres (100 mg) + 0.1 M BMITFI and (b) only 0.1 M EDOT + 0.1 M BMITFI in 10 mL acetonitrile. Quantum dot solar cells were assembled by using a CdS/ TiO_2 electrode as the photoanode, a PEDOT/ NiS_2 or a PEDOT film as the counter electrode and a solution of 0.1 M Na_2S in 3:7 v/v of deionized water: methanol was used as the electrolyte. I-V characteristics were measured under illumination using a 150 W LOT-Oriel Xenon short arc lamp ($\lambda > 300 \text{ nm}$) and the data was obtained using an Autolab 302 N Potentiostat/Galvanostat, operating in the linear sweep voltammetric mode between two set potentials. The intensity incident on the measuring cell was calibrated using a reference silicon solar cell traceable to NREL and it was set at approximately one sun (100 mW cm^{-2}). The incident light intensity was also reaffirmed by using a Newport power meter.

Table S1 Solar cell parameters for QDSCs with CdS/ TiO_2 -0.1 M Na_2S -CE configurations.

Counter electrode	V_{oc} (mV)	J_{sc} (mA cm^{-2})	FF (fill factor)	η (Efficiency, %)
PEDOT	682.8	4.65	0.39	1.238

Supporting information

PEDOT/NiS ₂	738.3	4.54	0.384	1.287
------------------------	-------	------	-------	-------